SOME ASPECTS OF PROCESSING EXTRATERRESTRIAL LIDAR DATA: CLEMENTINE, NEAR, MOLA

Gregory A. Neumann[1,2]

[1]Laboratory for Terrestrial Physics, NASA/Goddard Space Flight Center
[2]Department of Earth, Atmospheric and Planetary Sciences, Massachusetts Institute of Technology
neumann@tharsis.gsfc.nasa.gov

KEYWORDS: Laser altimetry, planetary mapping, topography, geolocation, crossover analysis

ABSTRACT

The increasing volume of planetary lidar data is creating global datasets of unprecedented resolution and accuracy, and presenting new challenges. From 1971-72, when three Apollo missions carried laser altimeters to the Moon, to the Mars Global Surveyor mission operating the MOLA instrument for nearly 1000 days, the number of planetary ranges has increased by more than 5 orders of magnitude, and accuracy by nearly 3 orders. Significant refinements to orbital and attitude knowledge result from the use of millions of altimetric crossover constraints.

1 INTRODUCTION

Table 1 shows the dramatic improvement in laser terrain mapping since the first use of lasers by the Apollo Orbiters. The NEAR Laser Rangefinder (NLR) returned 16 million ranges and the Mars Orbiter Laser Altimeter (MOLA) instrument returned over 600 million ranges, five orders of magnitude more than the first altimeters flown by the Apollo lunar orbiters. Over a time span of 25 years, this represents a doubling of yield every 18 months, similar to Moore's law for transistors! The Geoscience Laser Altimeter System and MultiBeam Laser Altimeter instruments are expected to increase yield and accuracy by another factor of 10.

This paper compares Clementine, Shuttle Laser Altimeter (SLA), NLR and MOLA from the perspective of data analysis and validation. Apollo, Clementine, SLA, NLR, and MOLA operations span nearly three decades. The small number of orbital lidar missions is surprising in view of their success and modest cost. Planetary terrain mapping depends on coverage, instrument calibration and performance, timing, pointing, and precise orbital analysis. We review each of these factors over the course of these missions. We then describe some of the unique characteristics of long duration laser altimetric missions, focusing on the geolocation of NLR and MOLA ranges.

1.1 Coverage

Despite numerous orbital missions, lunar topography remains poorly known at scales less than 100 km. Optical and radar ground-based mapping of landmarks is limited to the nearside and has only recently achieved good resolution [*Margot et al.*, 1999, and references therein]. High-resolution regional contour maps were created from Apollo metric camera stereo images, using control from laser altimeters, but coverage was modest. The Apollo laser transmitters were short-lived. Pulse width was controlled mechanically, and their flashlamp exciters required 16-32 s to recharge. In the low-inclination (26°) orbits used for landing approaches, only a limited region of terrain was sampled (Figure 3). Apollo 17's laser outlasted the others, enduring 12 revolutions as the command module grazed within a few kilometers of the surface. Had the astronauts persisted and the lasers not failed, orbital decay would soon have ended the missions.

Two decades later, Clementine [*Nozette et al.*, 1994], a joint mission of NASA and the Ballistic Missile Defense Organization, spent two months in a 5-hour eccentric lunar orbit, with a 400-km periapse placed first at 30°S, then 30°N. Clementine obtained useful lidar data from 284 of its revolutions [*Smith et al.*, 1997]. With a hardware limited maximum of 640 km, the moon was within lidar range for at most 30 minutes per orbit. The detector system shared optics with the camera and was poorly tuned for mapping, so that few laser shots were returned from rough terrain. Laser shots were interleaved with imaging sequences, limiting firing rate. Coverage was spotty at best in the rough topography of the lunar highlands, where the shot-to-shot variance exceeded 1 km [*Smith et al.*, 1997].

Clementine demonstrated new, efficient, diode-pumped laser technology. Its significance might have been less had the Mars Observer mission not been lost the previous year. The Mars Observer Laser Altimeter (MOLA) was a redesigned lunar altimeter (not surprisingly called LOLA) sharing heritage with Clementine, optimized for planetary mapping [*Zuber et al.*, 1992]. Lacking an immediate reflight, MOLA spares were assembled with ancillary electronics to create the Shuttle Laser Altimeter. SLA was a Hitchhiker payload on STS-72 and later on STS-85 [*Garvin et al.*,

Table 1. Laser Altimetry Missions[a]

Mission Name	Launch Date	Type	Firing Rate, Hz	Shots fired	Geolocated Ranges	Horizontal accuracy	Vertical precision	Vertical accuracy
Apollo 15, 16, 17	1971-1972	Ruby	0.06	7,080	5,140	30 km	4 m	400 m
Clementine	1994	Cr:Nd:YAG[b]	0.6	600,000	72,300	3 km	40 m	90 m
SLA-01	01/1996	Cr:Nd:YAG	10	3,000,000	1,203,000	40 m	0.75 m	2.78 m
SLA-02	08/1997	Cr:Nd:YAG	10	3,000,000	2,090,000	40 m	0.75 m	6.74 m
NLR	02/1996	Cr:Nd:YAG	1-2	20,000,000	15,868,304	20 m	0.31 m	10 m
MOLA	11/1996	Cr:Nd:YAG	10	675,000,000	583,000,000	100 m	0.38 m	1 m

[a]The number of geolocated ground returns does not necessarily reflect the instrument's ability to range. Spacecraft off-pointing, data loss, gaps in tracking, clouds, as well as range failure limit the altimetric product.

[b]Chromium:neodymium-doped yttrium-aluminum-garnet

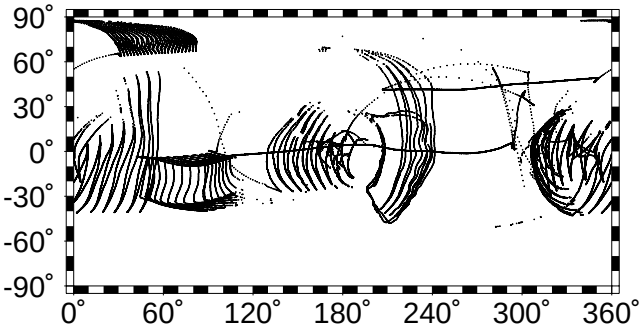

Figure 1. NLR coverage of 433 Eros on day 2000-111. Typically most of the coverage was acquired in rapid off-nadir scans.

1997, 1998]. SLA-01 and 2 demonstrated the effectiveness of orbital laser altimeters for terrestrial geodesy despite relatively short flights and the inconvenience of using the shuttles as an orbital platform. SLA-01 obtained excellent land and sea data between 28°N/S, and SLA-02 from 57°N/S. *Carabajal et al.* [1999] provides details of data processing and coverage.

NEAR-Shoemaker and Mars Global Surveyor (MGS) were launched successfully in 1996, carrying NLR and MOLA-2. Each achieved their planned orbits after some delay, but with all instruments performing well. NEAR orbited the asteroid 433 Eros for nearly one year before landing. Figure 1 shows a typical day's data acquired at 1 Hz at a range of 100 km. The NLR instrument [*Cole et al.*, 1997] had an 11 m spot size in the nominal 50 km orbit, and operated at ranges from 300 km to 17 m. Low-altitude orbits of 35 and 25 km radius allowed higher resolution mapping, with shots 3-4 m apart. NEAR-Shoemaker performed rapid scans and traverses for imaging purposes with NLR "riding along", ranging to nadir only a fraction of the time. Figure 2 shows the global dataset of observations. The coverage was highly nonuniform due to the asteroid's irregular shape and mission constraints. Data recovery was nearly perfect, with full attitude and timing reconstructions provided. Many track crossings were obtained.

The delayed MGS mission allowed limited coverage of the northern hemisphere of Mars in 1997-98. During aerobraking MOLA ranged intermittently from 170 km to 785 km in an elliptical orbit [*Zuber et al.*, 1998]. In mapping orbit, MOLA operated continuously at elevations of 365 to 430 km for a total of 26 months [*Smith et al.*, 2001b] before losing a critical oscillator signal on June 30, 2001. More than 98% of laser shots returned ground ranges. About 8% of ranges were unusable due to telemetry losses, attitude reconstruction gaps, and other events. The MGS orbital inclination of 92.7° allowed nadir coverage of 99.9% of the planet, with a few off-nadir observations of the poles. So many returns were obtained that in many regions topographic terrain models are better than Viking-era images [*Withers and Neumann*, 2001]. With shot spacing typically 300 m along track, nearly 50 profiles cross the equator for each degree of longitude (about 60 km). In some places on Mars, several profiles traverse a single square kilometer (Figure 4). Mapping was nominally in an 88-cycle near-repeat orbit, with a ground track offset that eventually transitioned from positive to negative. Some tracks overlapped, enabling direct temporal comparisons of topography between seasons [*Schmerr et al.*, 2001]. Most importantly the regular crossings of ascending and descending tracks provided many internal consistency checks.

1.2 Instrument performance and calibration

The Apollo altimeters were more than adequate for their primary purpose, giving ranges for photographs, with a precision of about 4 m. While the 15 MHz oscillator of Clementine's laser rangefinder was calibrated within 1 part in 10^5, or a few meters of range, only a 14-bit range count was returned, since full 16-bit hardware was not available on an accelerated development schedule. To reach a 640-km-distant target, ranges were quantized to 40 m, as illustrated in Fig-

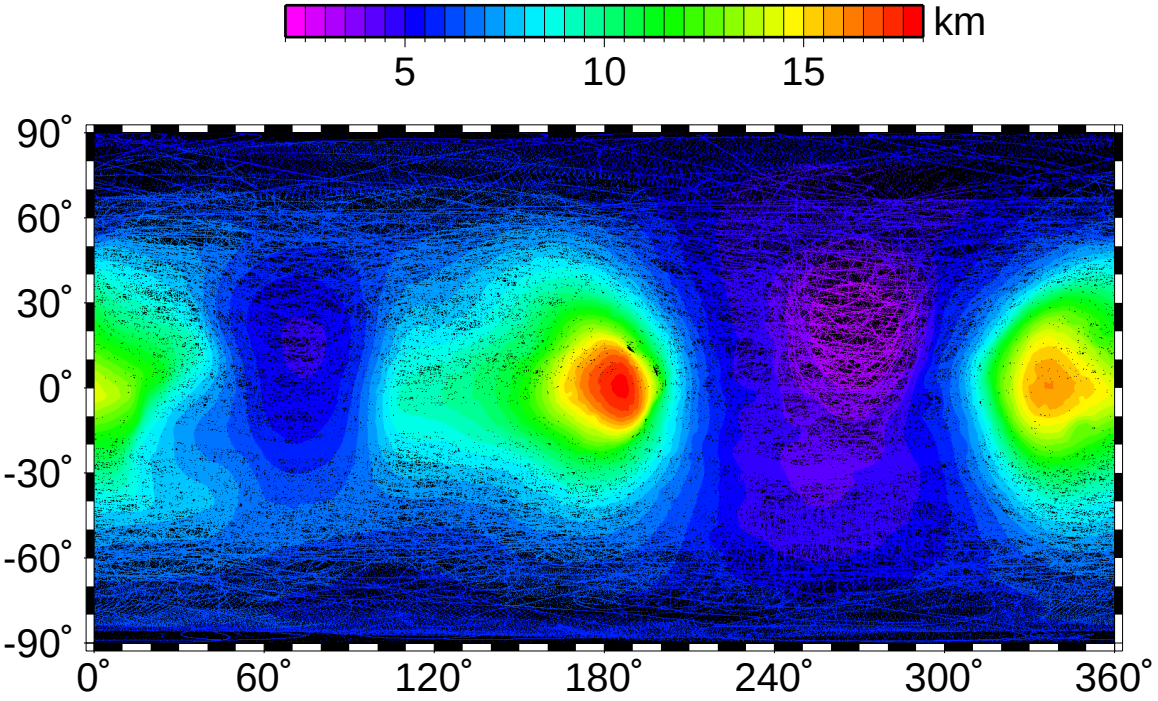

Figure 2. NLR altimetric coverage of asteroid 433 Eros. Regions lacking data shown in black.

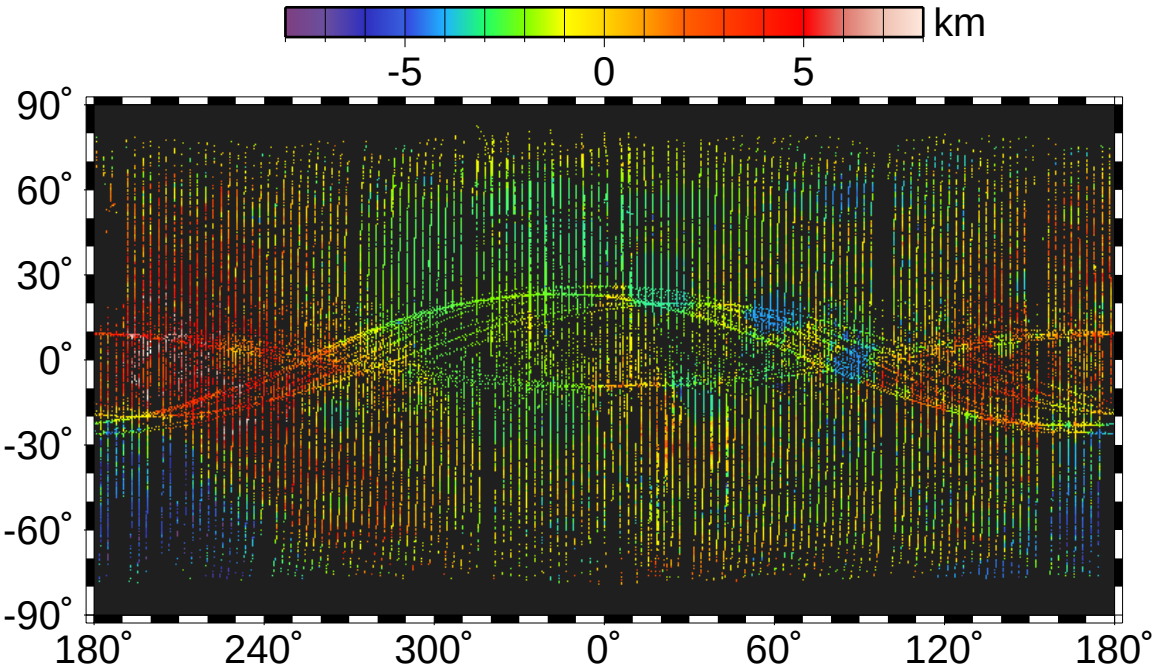

Figure 3. Lunar topographic coverage from Apollo orbiters and Clementine [*Smith et al.*, 1997].

ure 5. The laser could range at 8 Hz for about 1 minute until overheating. The only good 8-Hz profile taken under ideal conditions over smooth Mare terrain shows shot-to-shot variation of about 40 m. Comparison with a MOLA profile over level terrain (lower curve) shows that precision was limited due to quantization and electronic jitter.

Another problem was Clementine's low signal-to-noise ratio. Elevations had to be processed with a range-correlation filter to edit the nearly 50% noise triggers, and many errors remain. Finally, the orientation of the laser transmitter was uncertain. The laser was boresighted to a detector within the camera telescope, so that ranges were nominally pointed at spacecraft nadir, but the amount of offset was not known at the time of the analysis. Information obtained since from the

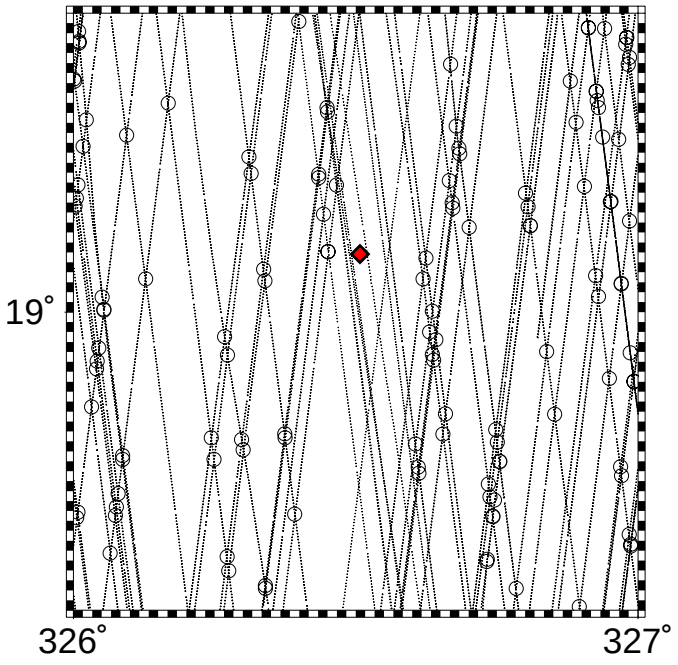

Figure 4. Coverage in a 1° by 1° area around the Pathfinder landing site (solid diamond) acquired by MOLA. Border markings are 1 minute (roughly 1 km). Individual shot elevations (crosses) are compared at crossovers (circles).

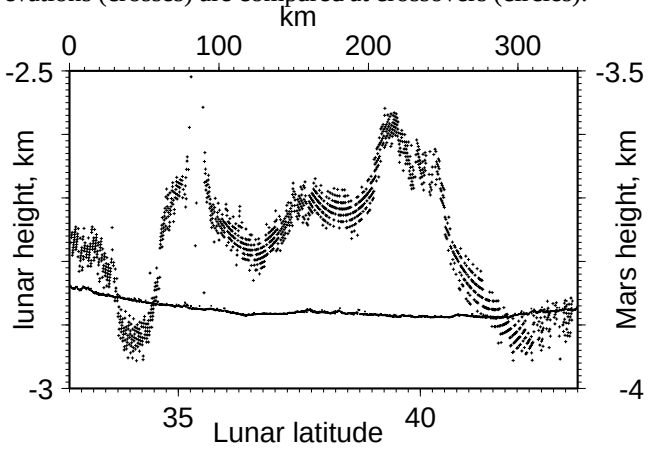

Figure 5. Clementine high-resolution rangefinder profile extending 340 km across northwest Mare Procellarum (crosses). Vertical exaggeration ∼400:1. MOLA profile 10061 across Amazonis Planitia, one of the flattest places in the solar system, shown for comparison.

SPICE archives at JPL shows a 5 mrad deviation in camera orientation along-track and 1 mrad across-track. This offset was also indicated by a comparison with ground-based radar interferometry [*Margot et al.*, 1999], showing a 3-km offset along-track.

NLR was rigorously calibrated, and drift of the instrument after launch was monitored via an optical delay fiber [*Cheng et al.*, 2000]. Ranging performance from shot-to-shot approached the limiting resolution of 31 cm, and noise was negligible at all but the lowest operating threshold. The largest single source of range error was due to pulse dilation on non-ideal target surfaces, or "range walk". Dilation causes the leading edge of a pulse to be detected early, introducing range bias as much as 6 m error on sloping terrain [*Zuber et al.*, 1997].

MOLA is a fully calibrated [*Abshire et al.*, 2000], all-terrain lidar with direct (leading edge of pulse) detection. MOLA pulse waveforms vary due to interaction with the surface of Mars, and their energy varies with atmospheric transmission and surface reflectivity. MOLA-2 addressed the issue of range walk by measuring the echo pulse width at a preset threshold, and the echo energy. Time of flight was corrected to the centroid of the pulse using half the measured pulse width. With this approach, calculated range errors due to detector noise were less than 1 m over slopes of up to 3°. This calibration enables unbiased comparison of measurements from different altitudes, laser outputs, and atmospheric conditions. The situation was complicated by the use of four parallel low-pass filters to maximize the probability of detection under all conditions, and the generally saturated condition of the detector over the unusually flat martian terrain seen in Figure 5. For saturated pulses, the pulse width measurement was unreliable. The leading-edge to centroid timing delay was estimated based on terrain slope, while interchannel calibration at the sub-meter level was obtained empirically [*Neumann et al.*, 2001].

The MOLA timing interval clock controls firing rate as well as range measurement. By monitoring the firing rate, an absolute calibration of range units over the course of the mission was obtained, adding to the stability of the range measurement. The calibration changed by several parts per million over the course of the mission [*Smith et al.*, 2001b], accelerating in the final weeks before the clock signal was lost.

By averaging over many shots, MOLA can measure temporal changes in the height of the Martian surface with decimeter precision. MOLA elevation measurements have recently been used to map 1-2 m seasonal changes due to the deposition and sublimation of CO_2 ice [*Smith et al.*, 2001a] associated with the planet's seasonal cycle of CO_2 exchange. Unfortunately in polar regions, many of MOLA's returned pulses were saturated, which greatly compromises the measurement of pulse energy. In some regions there may be significant unmodeled range walk due to albedo changes. A global 1064 nm albedo map being generated as part of the investigation will permit an improved estimate of echo pulse energy. This will enable a more accurate correction of range walk effects and therefore improve the ability to detect subtle patterns of topographic change in the polar regions.

1.3 Orbit determination

Orbital analysis during the Apollo era was crude by today's standards and the lunar gravity field was largely unknown. Many archives have been lost or contain only partial information. Position errors of 30 km or more were not uncom-

mon. Reanalysis of historical lunar tracking [*Lemoine et al.*, 1997] together with sophisticated force modeling reduced Clementine's orbital uncertainties to 10's of meters. Some improvement in orbits might be obtained from using gravity fields derived from Lunar Prospector [*Konopliv et al.*, 1998, 2001], but the issues with ranging accuracy mentioned earlier would remain.

SLA used a combination of Global Positioning Satellite (GPS) and Tracking/Data Relay Satellite System (TDRSS) together with TOPEX-Poseidon to TDRSS tracking [*Rowlands et al.*, 1997] to generate orbits with meter-level radial precision. Long-wavelength orbital errors remained but were masked by pointing uncertainty [*Luthcke et al.*, 2000].

Orbit determination for NEAR-Shoemaker at Eros remains problematic. The small gravitational pull of the body provided weak dynamic constraints, while tracking range data were biased by uncertainty in the asteroid ephemeris. Altimetry was required to constrain the orbits, as well as optical landmark tracking [*Yeomans et al.*, 1999; *Zuber et al.*, 2000]. Only partial altimetry were included in orbit solutions, using a low-degree shape model to provide an apriori constraint. Altimetric residuals were $\sim$60-110 m, depending on orbital phase. In this situation, much improvement may be gained from the use of crossovers, described in a following section.

MGS tracking was intermittent during aerobraking. Orbit solutions typically had 5-10 m errors, occasionally more. After reaching a circular mapping orbit, a period of tracking was dedicated to refining knowledge of the martian gravity field. The MGS orbital total position was subsequently determined to an accuracy of 1.7 m, and 0.3 m radially [*Lemoine et al.*, 1999]. Exceptions occurred when propulsive momentum desaturation occurred during long gaps in tracking and could not be adequately modeled. During these gaps, radial orbit error sometimes exceeded 20 m [*Neumann et al.*, 2001].

1.4 Timing bias estimation

Timing is another source of uncertainty in geolocation, since the spacecraft ephemeris is determined from Earth-based tracking. Clementine timing was corrupted by recurrent computer resets, and had to be corrected by as much as 32 seconds. Timing reconstruction was not available until more than a year after the mission ended. Thus an empirical approach to corrections was required for the analysis of the Laser Rangefinder data. Since in a polar orbit there were no crossing tracks and little other data, the only comparisons available were with nearby tracks taken during the second monthly mapping cycle over relatively smooth basins (cf. Figure 5). These revealed some mundane timing software issues and prompted a full timing reconstruction.

Global Positioning Satellites provide accurate timing in earth orbit, although SLA used the shuttle precision clock for a reference. The interface to this clock was problematic, and some time periods contained invalid tags [*Carabajal et al.*, 1999]. At the 1-2 AU distances to 433 Eros, time transfer is nontrivial. The NEAR-Shoemaker spacecraft was aided by solutions for times of cosmic gamma ray burst events observed by multiple platforms. Timing accuracy was within 100 ms, more than adequate for a slow-moving spacecraft. Instrument firing was synchronized to the spacecraft clock, and timing bias was not anticipated.

The MGS spacecraft clock had a small and stable rate of drift throughout the mission and was monitored, but was not tied to the Ultra-Stable Oscillator instrument which could have maintained millisecond accuracy. The MGS Project specified a worst-case 30 ms timing uncertainty, although it was typically better than 10 ms. The orbital velocity of MGS during aerobraking ranged from 3.3-4.5 km/s, and a 10 ms error in timing resulted in up to 16 m of vertical error in an eccentric orbit. During the aerobraking mission phase, an observation timing bias of 117 ms was estimated[*Rowlands et al.*, 1999], the cause of which remains unknown. In addition there was an attitude timing bias of 1.15 s, discussed below.

1.5 Attitude bias and uncertainty

Pointing bias and uncertainties must be minimized as far as possible in the space environment. The importance of this was seen in the context of Clementine. Star trackers provide the inertial reference, supplemented by attitude gyros. When performing maneuvers, trackers may lose lock, and knowledge degrades rapidly. The alignment of laser boresight with respect to star trackers is liable to change in flight, and may be perturbed by thermal distortion. Different approaches may be taken to improve attitude knowledge and minimize bias. For the SLA missions, a joint solution for alignment bias together with orbit determination was undertaken, using the oceans as a reference [*Luthcke et al.*, 2000]. Independent verification was provided by comparison with well-controlled terrestrial terrain models.

The NEAR-Shoemaker spacecraft provided attitude data at 1 Hz throughout the mission. NLR and cameras were aligned prior to flight along the X-axis with respect to the Spacecraft Bus Prime coordinate system. The Multi-spectral Imager (MSI) was able to verify its alignment through star observations, and variations were detected that appeared to correlate with instrument deck temperature. The coalignment of NLR with MSI could not be determined by directly imaging the laser spot, despite several attempts. Indirect measurements were obtained by observing the time at which ranges were lost as the imager scanned across the asteroid limb [*Cheng et al.*, 2001]. Further information was obtained by laboriously comparing images of boulders with altimetric features, providing a location within two camera pixels ($\sim$0.2 mrad). It became apparent that the instrument had shifted from its pre-flight orientation. The laser mounting was thermally better isolated than that of the camera. Alignment was therefore investigated independently for NLR in the course of altimetric processing, as described in Section 2.

MGS attitude reconstruction from Lockheed-Martin in Den-

ver was provided by the Project in the form of spacecraft quaternions at approximately 4-second intervals. During aerobraking, images were taken of various landmarks (e.g., the Face on Mars) by means of rapid off-nadir slews. These slews revealed a timing bias in the reconstruction of attitude data. Such delays can lead to substantial errors in geolocation due to the $\sim$1 mrad/s pitch motion of MGS as it tracks nadir. In nadir mapping, timing biases trade off with alignment bias, but are distinguishable in the altimetry taken during maneuvers. *Rowlands et al.* [1999] found a shift in boresight of approximately 0.024° (0.42 mrad) from preflight, primarily in the roll direction.

MGS telemetry transmitted attitude quaternions after onboard processing with a causal delay due to two-pole, recursive digital filter. The filter characteristics included a phase shift equivalent to 1.15 s delay at low frequencies. Upon commencement of mapping, the solar panels oscillated slowly as they tracked the sun. A 6-s notch filter with two additional poles was added to damp the oscillations. Calculations suggested that the mapping filter should have induced a 2.3 s delay. We found that the delay was the same as before the commencement of mapping, both during normal operation and during high-rate slews. This apparent contradiction with theory remains unresolved, but MOLA alignment continued to be monitored throughout the mission.

2 ALTIMETRIC CROSSOVERS

Abundant crossovers in lidar mapping provide a powerful constraint on orbital and attitude knowledge. During the course of the NLR investigation, over $\sim$16,000,000 altimetric points were acquired. Distinct orbital phases permitted observations over northern and southern hemispheres, using nadir and off-nadir observations. In order to assess their accuracy, $\sim$3,800,000 crossovers were analyzed. A shot point (x,y,z) in Cartesian space is expressed in polar coordinates. Two sequential shot points define a small track segment, parameterized by time. Crossovers occur at the intersection of two such segments projected onto a sphere. The radius r is linearly interpolated along each track. At each crossover we obtain the altimetric residual

$$d(t, t') = r(t) - r(t') \quad (1)$$

at a time-ordered pair of crossover times t, t', as well as the crossing latitude, longitude, and a pair of headings and slopes.

A local surface normal perpendicular to both segments is estimated in Cartesian coordinates. This unit normal vector represents the change in radius at the time of intersection resulting from an adjustment of the track in the X, Y, and Z directions. There are six adjustments, three per track, for each crossover residual. Such an underdetermined problem may be solved by constraining the adjustment to vary as a smooth function of time. Using the approach of *Neumann et al.* [2001], tracks were adjusted to minimize the crossover residual via least-squares. The effort to obtain a solution in this simplified approach depends only linearly on the number of crossovers considered and thus can handle a very large dataset. The adjustment is made in body-fixed coordinates, and does not truly represent a single error in orbit, range, timing, or alignment, but rather the combined effects of each.

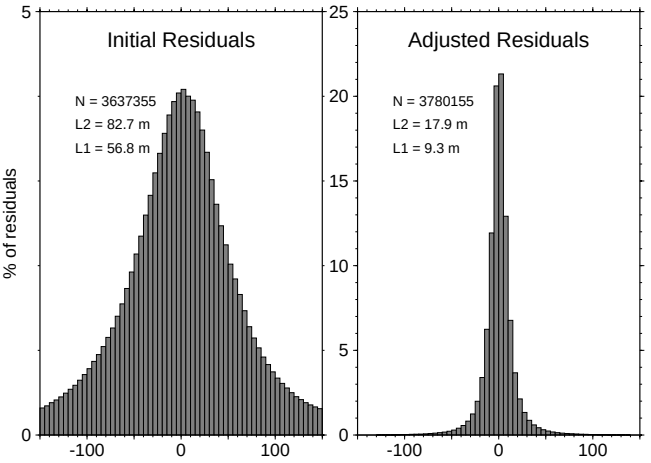

Figure 6. Initial and final crossover residuals for NLR altimetry, using a crossover adjustment with temporal resolution of four cycles per asteroid revolution. Residuals >200 m are edited.

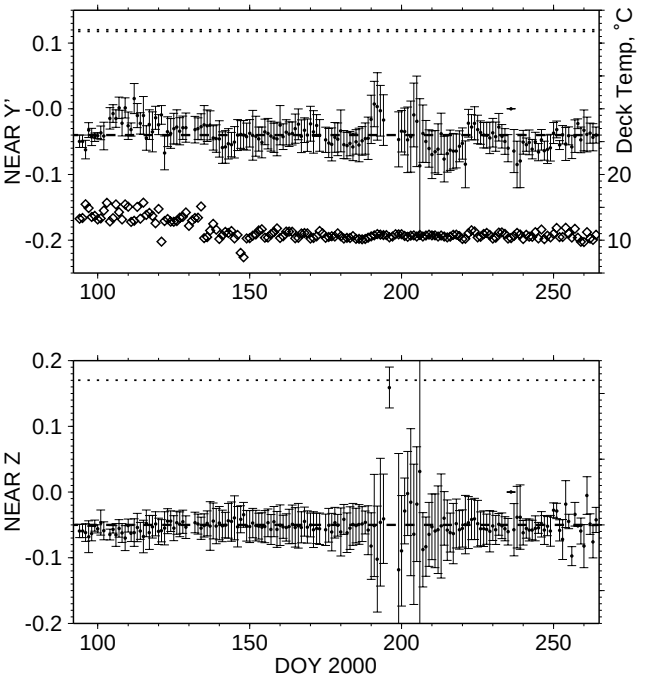

Figure 7. Boresight positions of crossovers after adjustment as a function of time. Error bars show the median daily dispersion about the median value. Dotted line shows initial value, while dashed lines show the nominal fit. Instrument deck temperatures (diamonds) declined early in the mission, but boresight did not appear to be correlated.

The relocated crossovers generally have smaller residuals. Figure 6 shows the initial and final residual after three iterations. An adjustment of four cycles per asteroid revolution reduced the RMS residuals d from 82.7 to 17.9 m, after excluding grossly mislocated data. A more typical measure of residual is the L_1 residual, the median absolute residual scaled to a normal distribution. Using this measure, a sixfold improvement in crossover error results from a quasi-periodic adjustment with a period of $\sim$1.25 hours. Obviously there are sources of error that vary more rapidly, but errors in the slow-moving NEAR orbit typically show up as errors at multiples of the 5-hour rotational period of Eros.

If one assumes that all but one of the sources of error are minor and randomly distributed, the relocated crossover indicates the amount of the chief source of error. For example, the position of the adjusted crossover in the instrument plane provides an estimate of true boresight direction. At each crossover the relocated range vector may be projected to the Y-Z plane (recall that instruments point in the platform X-direction). The median locus of these points shows the degree to which the boresight deviates from nominal, while the dispersion shows the relative contribution from other sources of error. Several iterations with improved boresight alignment successively reduce the crossover residual. Figure 7 shows the preflight boresight direction and daily averages of the apparent true boresight. No correlation with instrument deck temperature was seen. The spacecraft orbit remained illuminated by the Sun during all mission phases, keeping temperatures stable. The analysis used orbit solutions from day 2000-094 through day 264. The Euler angles obtained for the instrument were -0.04° about the Z-axis, and -0.05° about the Y-axis. These angles map a unit X-vector along the lidar boresight to the vector
`(0.999999376, -6.98131378E-04, 8.726645E-04)`^{T}
in the spacecraft frame. This boresight alignment offset was assumed for the remainder of the analysis. A final analysis using all 351 days of observations should refine this, but the uncertainty in pointing on a given day appears to be $\sim$0.01°, or 0.2 mrad.

Altimetric crossovers have been employed in the MOLA investigation to monitor the stability of pointing as well as orbital precision [*Neumann et al.*, 2001]. That study found that significant adjustments in three orthogonal directions were required to fit the crossover data. The regular mapping geometry allows the adjustments to be expressed in radial, along-track, and across-track components. Quasi-cyclic, once- and twice-per-rev adjustments dramatically reduced residuals. These cyclic errors were traced to unconstrained propulsive momentum dumps that perturbed the MGS orbit. A shorter-duration signal was seen when the spacecraft transitioned between night and day sides of Mars, inducing a thermal distortion of alignment between the MOLA beam and the inertial reference system.

Longer term drift can be characterized via daily averages. Figure 8 shows the average deviation from nominal alignment over the life of the mission. Some of the variation is correlated with spacecraft thermal environment as Mars' elliptical orbit circles the Sun. Drift in timing, spacecraft maneuvers, and gradual shift in spacecraft center-of-mass are also suspected.

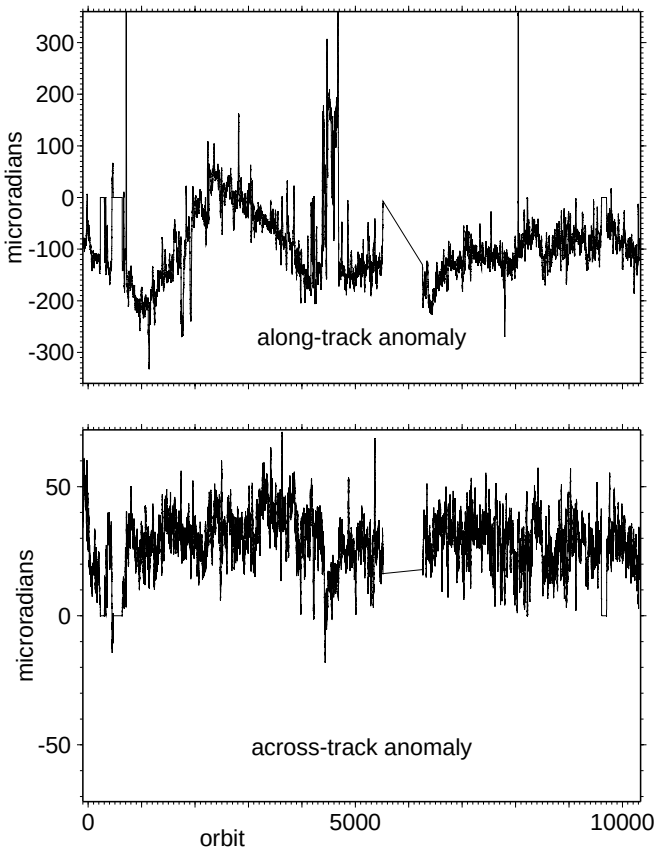

Figure 8. MOLA along-track and across-track misalignment as a function of orbit. Adjustment value from crossover analysis, averaged over one day. At a nominal altitude of 400 km, 100 μrad = 40 m. Some offsets result from targeting maneuvers affecting attitude knowledge, others from variations in beam alignment.

3 DISCUSSION

The Moon was the first extraterrestrial body to be ranged with lasers. The extant data are contaminated with instrument defects and other uncertainties, and are simply inadequate in quantity for detailed regional studies. Lunar topography awaits a fully calibrated, high-performance altimetric study by the next generation of laser altimeters.

The NLR and MOLA investigations have revealed the power of rigorous orbital processing within the GEODYN software system [*Rowlands et al.*, 1999] combined with full crossover analysis. The pointing bias on NLR has been characterized within 0.2 mrad and the topographic uncertainty reduced to $\sim$10 m via the use of crossovers [*Zuber et al.*, 2000]. An even better level of precision may be attainable given the capabilities of the NLR instrument.

MOLA had many more observations than any other mis-

sion, in a highly stable geometry, with more than 38 million topographic crossovers. Radial topographic accuracy of 1 m and horizontal position accuracy better than 100 m has been achieved. Where known positions of landers have been traversed, essentially identical topography is measured. Martian topography is referenced to an equipotential surface. Formal uncertainty in the martian geoid height, as currently defined by spherical harmonics to degree and order 60 [*Lemoine et al.*, 2001], is 1.8 m. At present the most uncertain element of martian cartography is the position of the prime meridian [*Davies et al.*, 1996], defined by the crater Airy-0, in inertial space.

Acknowledgments. Supported by the NASA Mars Exploration Program MOLA Investigation. The Generic Mapping Tools software [*Wessel and Smith*, 1998] greatly assisted the analysis.

REFERENCES

Abshire, J. B., X. Sun, and R. S. Afzal, Mars Orbiter Laser Altimeter: Receiver model and performance analysis, *Appl. Opt.*, *39*, 2440–2460, 2000.

Carabajal, C. C., D. J. Harding, S. B. Luthcke, W. Fong, S. C. Rowton, and J. J. Frawley, Processing of Shuttle Laser Altimeter range and return return pulse data in support of SLA-02, *International Archives of Photogrammetry and Remote Sensing*, *32*, 65–72, 1999.

Cheng, A. F., T. D. Cole, M. T. Zuber, Y. Guo, and F. Davidson, Inflight calibration of the Near-Earth Asteroid Rendezvous Laser Rangefinder, *Icarus*, *148*, 572–576, 2000.

Cheng, A. F., et al., Laser altimetry of small-scale features on 433 Eros from NEAR-Shoemaker, *Science*, *292*, 488–491, 2001.

Cole, T. D., M. T. Boies, A. F. C. A. S. El-Dinary, M. T. Zuber, and D. E. Smith, The Near Earth Asteroid Rendezvous laser altimeter, *Space Sci. Rev.*, *82*, 217–253, 1997.

Davies, M. E., et al., Report of the IAU/IAG/COSPAR working group on cartographic coordinates and rotational elements of the planets and satellites: 1994, *Cel. Mech. and Dynam. Astron*, *63*, 127–148, 1996.

Garvin, J. B., J. L. Bufton, J. B. Blair, S. B. Luthcke, J. J. Frawley, and J. A. Marshall, Observations of the Earth's topography from the Shuttle Laser Altimeter (SLA): Laser pulse echo recovery measurements of terrestrial surfaces, in *Proc. European Geophys. Soc. Mtg.*, Vienna, 1997.

Garvin, J. B., J. L. Bufton, J. B. Blair, D. Harding, S. B. Luthcke, J. J. Frawley, and D. D. Rowlands, Observations of the Earth's topography from the Shuttle Laser Altimeter (SLA): Laser pulse echo recovery measurements of terrestrial surfaces, *Phys. Chem. Earth*, *23*, 1053–1068, 1998.

Konopliv, A. S., A. Binder, L. Hood, A. Kucinskas, W. L. Sjogren, and J. G. Williams, Gravity field of the moon from lunar prospector, *Science*, *281*, 1476–1480, 1998.

Konopliv, A. S., A. Binder, L. Hood, A. Kucinskas, W. L. Sjogren, and J. G. Williams, Gravity field of the moon from lunar prospector, *submitted to Journal of Geophysical Research*, 2001.

Lemoine, F. G., D. E. Smith, M. T. Zuber, G. A. Neumann, and D. D. Rowlands, A 70th degree and order lunar gravity model from Clementine and historical data, *J. Geophys. Res.*, *102*, 16,339–16,359, 1997.

Lemoine, F. G., D. D. Rowlands, D. E. Smith, D. S. Chinn, D. E. Pavlis, S. B. Luthcke, G. A. Neumann, and M. T. Zuber, Orbit determination for Mars Global Surveyor during mapping, in *AAS/AIAA Astrodynamics Specialist Conference, Girdwood, Alaska, 16-19 August 1999*, pp. 99–328, 1999.

Lemoine, F. G., D. E. Smith, D. D. Rowlands, M. T. Zuber, G. A. Neumann, D. S. Chinn, and D. E. Pavlis, An improved solution of the gravity field of Mars (GMM-2B) from Mars Global Surveyor, *J. Geophys. Res.*, *in press*, 2001.

Luthcke, S. B., D. D. Rowlands, J. J. McCarthy, E. Stoneking, and D. E. Pavlis, Spaceborne laser-altimeter-pointing bias calibration from range residual analysis, *J. Spacecr. Rockets*, *37*, 374–384, 2000.

Margot, J.-L., D. B. Campbell, R. F. Jurgens, and M. A. Slade, The topography of Tycho Crater, *J. Geophys. Res.*, *104*, 11,875–11,882, 1999.

Neumann, G. A., D. D. Rowlands, F. G. Lemoine, D. E. Smith, and M. T. Zuber, Crossover analysis of Mars Orbiter Laser Altimeter data, *J. Geophys. Res.*, *in press*, 2001.

Nozette, S., et al., The Clementine mission to the moon: Scientific overview, *Science*, *266*, 1835–1839, 1994.

Rowlands, D. D., S. B. Luthcke, J. A. Marshall, C. M. Cox, R. G. Williamson, and S. C. Rowton, Space shuttle precision orbit determination in support of SLA-1 using TDRSS and GPS tracking data, *J. Astro. Sci.*, *45*, 113–129, 1997.

Rowlands, D. D., D. E. Pavlis, F. G. Lemoine, G. A. Neumann, and S. B. Luthcke, The use of crossover constraint equations derived from laser altimetry in the orbit determination of Mars Global Surveyor, *Geophys. Res. Lett.*, *26*, 1191–1194, 1999.

Schmerr, N., G. A. Neumann, S. E. H. Sakimoto, and J. B. Garvin, Seasonal changes in thickness of martian crater deposits from the Mars Orbiter Laser Altimeter, *Eos Trans. AGU*, *82*, *Fall Meet. Suppl.*, to appear, 2001.

Smith, D. E., M. T. Zuber, G. A. Neumann, and F. G. Lemoine, Topography of the Moon from the Clementine lidar, *J. Geophys. Res.*, *102*, 1591–1611, 1997.

Smith, D. E., M. T. Zuber, and G. A. Neumann, Seasonal variations of snow depth on Mars, *submitted to Science*, 2001a.

Smith, D. E., et al., Mars Orbiter Laser Altimeter: Experiment summary after the first year of global mapping of Mars, *J. Geophys. Res.*, *in press*, 2001b.

Wessel, P., and W. H. F. Smith, New, improved version of Generic Mapping Tools released, *Eos Trans. AGU*, *79*, 579, 1998.

Withers, P., and G. A. Neumann, Enigmatic northern plains of Mars, *Nature*, *410*, 651, 2001.

Yeomans, D. K., et al., Estimating the mass of asteroid 433 Eros during the NEAR spacecraft flyby, *Science*, *285*, 560–561, 1999.

Zuber, M. T., D. E. Smith, S. C. Solomon, D. O. Muhleman, J. W. Head, J. B. Garvin, J. B. Abshire, and J. L. Bufton, The Mars Observer Laser Altimeter investigation, *J. Geophys. Res.*, *97*, 7781–7797, 1992.

Zuber, M. T., D. E. Smith, A. F. Cheng, and T. D. Cole, The NEAR laser ranging investigation, *J. Geophys. Res.*, *102*, 23,761–23,773, 1997.

Zuber, M. T., D. E. Smith, R. J. Phillips, S. C. Solomon, W. B. Banerdt, G. A. Neumann, and O. Aharonson, Shape of the northern hemisphere of Mars from the Mars Orbiter Laser Altimeter (MOLA), *Geophys. Res. Lett.*, *25*, 4393–4396, 1998.

Zuber, M. T., et al., The shape of 433 Eros from the NEAR-Shoemaker Laser Rangefinder, *Science*, *289*, 2097–2101, 2000.